www.ijemr.net ISSN (ONLINE): 2250-0758, ISSN (PRINT): 2394-6962

Volume-5, Issue-3, June-2015

International Journal of Engineering and Management Research

Page Number: 436-443

Thermoelastic Analysis of Variable Thickness FGM Rotating Disk by Finite Element Method

Amit Kumar Thawait [1], Lakshman Sondhi [2]

[1]Department of Mechanical Engineering, Shri Shankaracharya Technical Campus, SSGI. Bhilai (C.G.), INDIA

[2]Department of Mechanical Engineering, Shri Shankaracharya Technical Campus, SSGI, Bhilai, (C.G.), INDIA

ABSTRACT

In this paper Elastic and thermal stress analysis of FGM rotating disks are done. The disk is made up of functionally graded material, whose mechanical and physical properties vary exponentially in radial direction. Uniform as well as variable thickness (concave, linear and convex) rotating disks subjected to linear temperature field are formulated and analyzed. The disk is modeled as axisymmetric body and 8-noded quadrilateral element is used for finite element formulation. Resulting displacement and stresses induced in the disks due to centrifugal force and uneven temperature distribution are evaluated in ANSYS Mechanical APDL and compared.

Key words—Thermoelastic analysis; Functionally graded material (FGM); Variable thickness rotating Disk; Finite element method (FEM); ANSYS Mechanical APDL.

I. INTRODUCTION

Rotating disks are of practical concern in many fields of engineering, such as marine, mechanical and aerospace industry including gas turbines, gears, turbo-machinery, flywheel systems and centrifugal compressors. The stresses due to centrifugal load can have important effects on their strength and safety. Thus, control and optimization of stress and displacement fields can help to reduce the overall payload in industries.

In some application such as gas turbines the rotating disk experiences mechanical as well as thermal loadings. Due to non uniform temperature distribution thermal stresses are generated which reduces the limit speed or maximum speed of the disk.

Material properties and thickness of the disk are two very important parameters to control the maximum stress induced. Disks made up of functionally graded materials and variable thickness cross section have significant stress reduction over the disk made up of homogeneous material and of constant thickness profile. Therefore a higher limit speed is permissible for FGM disks of variable thickness cross section.

Many researchers have worked on limit speed and thermoelastic stress analysis of rotating disks by analytical as well as approximate methods. J.N. Sharma, Dinkar Sharma, Sheo Kumar[1] have worked on the finite element analysis of thermoelastic stresses, displacements and strains in a thin circular functionally graded material (FGM) disk subjected to mechanical as well as thermal loads. Hasan Callioglu, Metin Sayer, Ersin Demir [2] has analyzed functionally graded rotating annular disk subjected to internal pressure and various temperature distributions such as uniform temperature, linearly increasing and decreasing temperature in radial direction. An analytical thermoelasticity solution for a disc made of functionally graded materials (FGMs) is presented by Hasan Callioglu [3]. Ashraf M. Zenkour and Daoud S. Mashat[4] have found stress function of a rotating variable-thickness annular disk using exact and numerical Methods. The disk has free boundary condition and Runge-Kutta numerical method was used for numerical solution. Hassan Zafarmand, Mehran Kadkhodayan [5] have found the nonlinear elasticity solution of functionally graded nanocomposite rotating thick disks with variable thickness reinforced with single-walled carbon nanotubes (SWCNTs). The governing nonlinear equations are based on the axisymmetric theory of elasticity with the geometric nonlinearity in axisymmetric complete form. The nonlinear graded finite element method (NGFEM) based on Rayleigh–Ritz energy formulation with the Picard iterative scheme is employed to solve the nonlinear equations. The solution is considered for four different thickness profiles, namely constant, linear, concave and convex. Mohammad Zamani Nejad and Parisa Fatehi [6] have worked to obtain the exact elastoplastic deformations and stresses of rotating thick walled cylindrical pressure vessels made of functionally graded materials (FGMs) under plane strain condition. The plastic stresses and deformations are obtained, using

Tresca's yield condition, and its flow rule under the assumption of perfectly plastic material behavior. Hassan Zafarmand and Behrooz Hassani [7] have found elasticity solutions of two-dimensional functionally graded rotating annular and solid disks with variable thickness. Axisymmetric conditions are assumed for the two-dimensional functionally graded disk. The graded finite element method (GFEM) has been applied to solve the equations. Abdur Rosyid, Mahir Es-Saheb and Faycal Ben Yahia [13] has worked on Stress Analysis of Nonhomogeneous Rotating Disc with Arbitrarily Variable Thickness Using Finite Element Method. Power law, sigmoid and exponential distribution is considered for the volume fraction distributions of the functionally graded plates and the work includes parametric studies performed by varying volume fraction distributions and boundary conditions

II. GEOMETRIC MODELING

For annular disk [12]

$$h(r) = h_0\left[1 - q\left(\frac{r}{b}\right)^m\right] \quad \ldots(1)$$

where

$h(r) = thickness\ of\ the\ disk\ at\ radius\ r$
$a = inner\ radius = 15\ mm$
$b = outer\ radius = 150\ mm$
$m = 1\ for\ linearly\ varying\ thickness\ profile$
$= 0.5\ for\ concave\ thickness\ profile$
$= 2\ for\ convex\ thickness\ profile$
$q = 0\ for\ uniform\ thickness$
$= 0.7\ for\ variable\ thicknss$
$h_0 = 7.73\ for\ convex\ thickness\ profile$
$= 9.21\ for\ linear\ thickness\ profile$
$= 11.51\ for\ concave\ thickness\ profile$

III. MATERIAL MODELING

The disk is of Al_2O_3/Al functionally graded material and has exponentially varying material properties [13]. The young's modulus of elasticity, density and co-efficient of thermal expansion has following exponential variation:

$$E(r) = E_0 e^{\beta r} \quad \ldots(2)$$

$$\rho(r) = \rho_0 e^{\gamma r} \quad \ldots(3)$$

$$\alpha(r) = \alpha_0 e^{\mu r} \quad \ldots.(4)$$

Where

$$E_0 = E_A e^{-\beta a}$$
$$\rho_0 = \rho_A e^{-\gamma a}$$
$$\alpha_0 = \alpha_A e^{-\mu a}$$
$$\beta = \frac{1}{a-b} ln\left(\frac{E_A}{E_B}\right)$$
$$\gamma = \frac{1}{a-b} ln\left(\frac{\rho_A}{\rho_B}\right)$$
$$\mu = \frac{1}{a-b} ln\left(\frac{\alpha_A}{\alpha_B}\right)$$

a and b are inner and outer radius, E_A, E_B, are young's modulus of elasticity for Al and Al_2O_3 while ρ_A and ρ_B are densities for Al and Al_2O_3 respectively. The inner surface of the disk (r = a) consists of 100% material A that is Al whereas the outer surface of the disk (r = b) is 100% material B that is Al_2O_3, Properties of Al and Al_2O_3 are shown in table I.

Table 1
Mechanical properties of Al and Al_2O_3

Material	E (MPa)	ρ (g/cm^3)	α (/ ^{0}C)
Al	71	2.70	23.1×10^{-6}
Al_2O_3	380	0.96	8.0×10^{-6}

IV. FINITE ELEMENT MODELING

A. Formulation

For axisymmetric problem, an (r-z) plane (analogous to x-y plane for plane elasticity) can be considered. Four independent nonzero strains exist in axisymmetric problems [11]:

In standard finite element notation, strain displacement relationship can be written as

$$\{\varepsilon\} = [B]\{\delta\}^e \quad \ldots(5)$$

Where [B] is strain displacement relation matrix which depends on element taken and contains derivatives of shape functions.

Due to the non uniform temperature distribution, a thermal strain ε_T acts on the disk equally in all direction:

$$\varepsilon_T = \alpha(r)T(r) \quad \ldots(6)$$

where α(r) is the co-efficient of thermal expansion as a function of radius r.

Thus the total strain is given by

$$\varepsilon_{Total} = e + \varepsilon_T \quad \ldots(7)$$

where e is the elastic strain.

From 3-D hooks law, component of total strain in radial, circumferential and axial direction is given by

$$\varepsilon_r = \frac{1}{E}(\sigma_r - \nu\sigma_\theta - \nu\sigma_z) + \alpha(r)T(r) \quad \ldots(8)$$

$$\varepsilon_\theta = \frac{1}{E}(\sigma_\theta - \nu\sigma_r - \nu\sigma_z) + \alpha(r)T(r) \quad \ldots(9)$$

$$\varepsilon_z = \frac{1}{E}(\sigma_z - \nu\sigma_\theta - \nu\sigma_r) + \alpha(r)T(r) \quad \ldots(10)$$

By solving above three equations, stress strain relationship can be obtained as follows:

$$\sigma_r = \frac{E(r)}{(1-2\nu)(1+2\nu)}[(1-\nu)\varepsilon_r + \nu\varepsilon_z + \nu\varepsilon_\theta] - \frac{E(r)\alpha(r)T(r)}{1-2\nu}$$

...(11)

Similarly axial and circumferential stress can also be obtained.

In standard finite element matrix notation above stress strain relations can be written as:

$$\{\sigma\} = [D(r)](\{\varepsilon\} - \{\varepsilon\}^0) + \{\sigma\}^0 - \{\sigma_T\} \quad \ldots(12)$$

Where

$$\{\sigma\} = \begin{Bmatrix} \sigma_r \\ \sigma_\theta \\ \sigma_z \\ \tau_{rz} \end{Bmatrix}$$

$$D(r) = \frac{(1-\nu)E(r)}{(1+\nu)(1-2\nu)} \begin{bmatrix} 1 & \frac{\nu}{(1-\nu)} & \frac{\nu}{(1-\nu)} & 0 \\ \frac{\nu}{(1-\nu)} & 1 & \frac{\nu}{(1-\nu)} & 0 \\ \frac{\nu}{(1-\nu)} & \frac{\nu}{(1-\nu)} & 1 & 0 \\ 0 & 0 & 0 & \frac{1-2\nu}{2(1-\nu)} \end{bmatrix}$$

$$\{\varepsilon\} = \begin{Bmatrix} \varepsilon_r \\ \epsilon_\theta \\ \varepsilon_z \\ \gamma_{rz} \end{Bmatrix}$$

$$\{\sigma_T\} = \frac{E(r)\alpha(r)T(r)}{1-2\nu} \begin{Bmatrix} 1 \\ 1 \\ 1 \\ 0 \end{Bmatrix}$$

D(r) is a function of radius r and $\{\sigma\}^0$ and $\{\varepsilon\}^0$ are initial stress and strain. Taking initial stress and strain zero, equation (16) reduces to

$$\{\sigma\} = [D(r)]\{\varepsilon\} - \{\sigma_T\} \quad ...(13)$$

Using the Principle of stationary total potential (PSTP) element stiffness matrix $[K]^e$ and element load vector $\{f\}^e$ are obtained as

$$[K]^e = \int_V [B]^T [D(r)][B]\ dv \quad ...(14)$$

$$\{f\}^e = \int_V \frac{1}{2}[B]^T\{\sigma_T\}\ dv + \int_V [N]^T\{q_v\}\, dv \quad ...(15)$$

The system level equation is given by

$$[K]\{\delta\} = \{F\} \quad ...(16)$$

where

$$[K] = \sum_{n=1}^{N} [K]^e = Globel\ Stiffness\ matrix$$

$$\{F\} = \sum_{n=1}^{N} [f]^e = Globel\ load\ vector$$

N = no. of elements.

The summation indicates assembly of individual elemental matrices following the standard procedure of assembly.

B. Calculation of elemental displacement vector, stiffness matrix, element force vector, stress and strain for 8- node quadrilateral element:

- ***Element displacement vector*** is given by

$$\{\varphi\} = [N]\{\delta\} \quad ...(17)$$

where

$$\{\varphi\} = \begin{Bmatrix} u \\ v \end{Bmatrix} = \text{element displacement vector}$$

$$[N] = \begin{bmatrix} N_1 & 0 & N_2 & 0 & \ldots. & N_8 & 0 \\ 0 & N_1 & 0 & N_2 & \ldots. & 0 & N_8 \end{bmatrix}$$

$$= matrix\ of\ linear\ shape\ functions$$

$$\{\delta\} = \begin{Bmatrix} u_1 \\ v_1 \\ u_2 \\ v_2 \\ \ldots. \\ \ldots. \\ u_8 \\ v_8 \end{Bmatrix} = element\ nodal\ displacement\ vector$$

- ***Element strain*** is given by [7]:

$$\{\varepsilon\} = [B]\{\delta\}^e \quad ...(18)$$

Where

$$\{\varepsilon\} = \begin{Bmatrix} \varepsilon_r \\ \varepsilon_\theta \\ \varepsilon_z \\ \gamma_{rz} \end{Bmatrix}$$

$$[B] = [B_1] \times [B_2] \times [B_3]$$

$$[B_1] = \begin{bmatrix} 1 & 0 & 0 & 0 & 0 \\ 0 & 0 & 0 & 0 & 1 \\ 0 & 0 & 0 & 1 & 0 \\ 0 & 1 & 1 & 0 & 0 \end{bmatrix}$$

$$[B_2] = \begin{bmatrix} \frac{J_{22}}{|J|} & \frac{-J_{12}}{|J|} & 0 & 0 & 0 \\ \frac{-J_{21}}{|J|} & \frac{J_{11}}{|J|} & 0 & 0 & 0 \\ 0 & 0 & \frac{J_{22}}{|J|} & \frac{-J_{12}}{|J|} & 0 \\ 0 & 0 & \frac{-J_{21}}{|J|} & \frac{J_{11}}{|J|} & 0 \\ 0 & 0 & 0 & 0 & 1 \end{bmatrix}$$

$$[B_3] = \begin{bmatrix} \frac{\partial N_1}{\partial \xi} & 0 & \frac{\partial N_2}{\partial \xi} & 0 & \ldots. & \frac{\partial N_8}{\partial \xi} & 0 \\ \frac{\partial N_1}{\partial \eta} & 0 & \frac{\partial N_2}{\partial \eta} & 0 & \ldots. & \frac{\partial N_8}{\partial \eta} & 0 \\ 0 & \frac{\partial N_1}{\partial \xi} & 0 & \frac{\partial N_2}{\partial \xi} & \ldots. & 0 & \frac{\partial N_8}{\partial \xi} \\ 0 & \frac{\partial N_1}{\partial \eta} & 0 & \frac{\partial N_2}{\partial \eta} & \ldots. & 0 & \frac{\partial N_8}{\partial \eta} \\ \frac{N_1}{r} & 0 & \frac{N_2}{r} & 0 & \ldots. & \frac{N_8}{r} & 0 \end{bmatrix}$$

and [J] = Jacobian matrix

$$[J] = \begin{bmatrix} \sum_{i=1}^{8} \frac{\partial N_i}{\partial \xi} r_i & \sum_{i=1}^{8} \frac{\partial N_i}{\partial \xi} z_i \\ \sum_{i=1}^{8} \frac{\partial N_i}{\partial \eta} r_i & \sum_{i=1}^{8} \frac{\partial N_i}{\partial \eta} z_i \end{bmatrix}$$

$$N_1 = \left(\frac{1}{4}\right)(1-\xi)(1-\eta)(-1-\xi-\eta)$$

$$N_2 = \left(\frac{1}{4}\right)(1+\xi)(1-\eta)(-1+\xi-\eta)$$

$$N_3 = \left(\frac{1}{4}\right)(1+\xi)(1+\eta)(-1+\xi+\eta)$$

$$N_4 = \left(\frac{1}{4}\right)(1-\xi)(1+\eta)(-1-\xi+\eta)$$

$$N_5 = \left(\frac{1}{2}\right)(1-\xi^2)(1-\eta)$$
$$N_6 = \left(\frac{1}{2}\right)(1+\xi)(1-\eta^2)$$
$$N_7 = \left(\frac{1}{2}\right)(1-\xi^2)(1+\eta)$$
$$N_8 = \left(\frac{1}{2}\right)(1-\xi)(1-\eta^2)$$

- ***Element stiffness matrix is*** given by

$$[K]^e = \int_V [B]^T [D(r)][B]\ dv \quad ...(19)$$

or

$$[K]^e = \iint [B]^T [D(r)][B]\ t dx dy \quad ...(20)$$

or

$$[K]^e = \int_{-1}^{1}\int_{-1}^{1} [B]^T [D(r)][B]\ t|J| d\xi d\eta \quad ...(21)$$

For an axisymmetric element $t=2\pi r$ therefore

$$[K]^e = 2\pi \int_{-1}^{1}\int_{-1}^{1} [B]^T [D(r)][B]\ r|J| d\xi d\eta \quad ...(22)$$

- ***Element force vector*** is given by

$$\{f\}^e = \int_V \frac{1}{2}[B]^T\{\sigma_T\}\ dv + \int_V [N]^T\{q_v\}\ dv \quad ...(23)$$

or

$$\{f\}^e = \iint \frac{1}{2}[B]^T\{\sigma_T\}\ t dx dy + \iint [N]^T\{q_v\} t dx dy \quad ...(24)$$

or

$$\{f\}^e = \int_{-1}^{1}\int_{-1}^{1} \frac{1}{2}[B]^T\{\sigma_T\}\ t|J| d\xi d\eta + \int_{-1}^{1}\int_{-1}^{1} [N]^T\{q_v\} t|J| d\xi d\eta \quad ...(25)$$

For an axisymmetric element $t=2\pi r$ therefore

$$\{f\}^e = 2\pi \int_{-1}^{1}\int_{-1}^{1} \frac{1}{2}[B]^T\{\sigma_T\}\ r|J| d\xi d\eta + 2\pi \int_{-1}^{1}\int_{-1}^{1} [N]^T\{q_v\} r|J| d\xi d\eta \quad ...(26)$$

- ***Elemental stress*** is given by

$$\{\sigma\} = [D(r)]\{\varepsilon\} - \{\sigma_T\} \quad ...(27)$$

C. Boundary conditions

- **Constraint boundary conditions:**

In an axisymmetric model rigid body motion in the x and z directions does not need to be constrained because it is controlled by the definition of axisymmetric elements [10]. However, at least one node must be constrained to prevent rigid body motion in the y-direction. Symmetry boundary condition is applied at the bottom edge of the half cross section of the disk. Inner surface is fixed along radial direction and outer surface is free.

Other constraints are also applied based on the boundary conditions such as fixed, free or simply supported at inner or outer radius etc. [8]

- **Inertial boundary condition:**

The disk has a uniform angular velocity of 1 rad/s which causes centrifugal force on the disk. For all elements body force vector due to rotation is given by:

$$\{q_v\} = \begin{Bmatrix} \rho(r)\omega^2 r \\ 0 \end{Bmatrix} \quad ...(28)$$

where $\rho(r)\omega^2 r =$ *centrifugal force due to rotation of the disk*

- **Thermal boundary conditions:**

The equation of linear temperature field is given by

$$T(r) = (T_a - T_0) + (T_b - T_a)\frac{(r-a)}{(b-a)} \quad ...(29)$$

where

$T_0 = reference\ temperaure = 0^0 C$

$T(r) = temperature\ at\ radius\ r, above\ the\ reference\ temperature\ T_0.$

$T_a = inner\ surface\ temperaure = 20^0 C$

$T_b = outer\ surface\ temperaure = 100^0 C$

In annular disk temperatures at inner and outer radius is fixed that is

$$at\ r = a, T(r) = T_a$$
$$at\ r = b, T(r) = T_b$$

1. Uniform disk

V. RESULTS AND DISCUSSION

A. Validation: The data of a functionally graded thin rotating disk [7] is used and the problem is modeled and analyzed in ANSYS. The inner and outer radii of the disk are a = 40mm and b = 100mm, and the thickness of the disk is 2.5 mm. The elasticity modulus and density vary in the r direction as below:

$$E(r) = E_0\left(\frac{r}{b}\right)^n$$
$$\rho(r) = \rho_0\left(\frac{r}{b}\right)^n$$

where E_0= 72 GPa, ρ_0= 2,800 kg/m^3 and the angular velocity is ω = 1,570.8 Rad/s. Poisson's ratio is taken 0.3. The boundary condition is free on both the inner and outer surfaces.

Figure 1 shows the comparison of current work with reference [7], results of current work are in good agreement with pre analyzed results of literature.

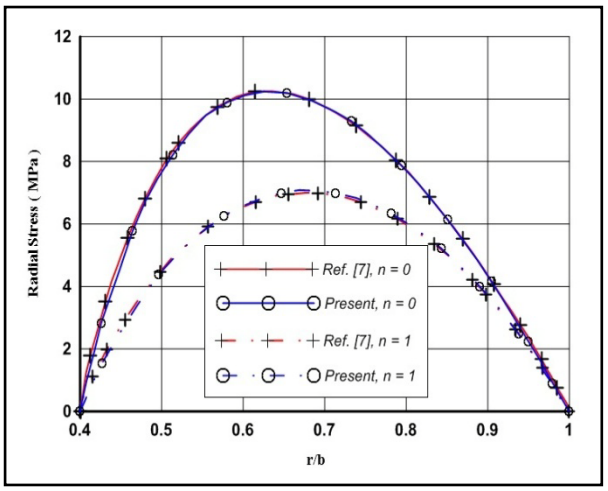

Figure 1: Comparison of current work with reference [7]

B. Results of current work: Fig 2 to Fig. 13 shows the variation of radial displacement, radial stress and circumferential stress for uniform, concave, linear and convex thickness disk respectively along the radial direction. Fig. 14 to 16 shows the comparison of the radial displacement, radial stress and circumferential stress. It is found that uniform thickness disk has a higher displacement and stresses as compared to variable thickness disk.

1. Uniform disk

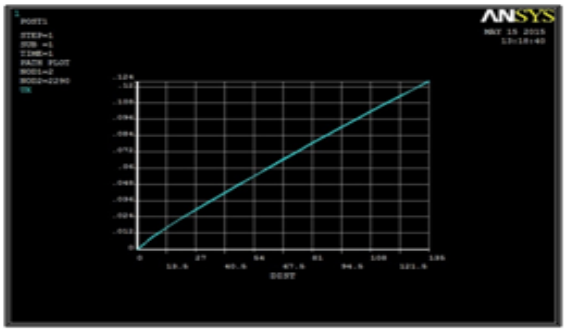

Figure 2: Variation of radial displacement for uniform disk

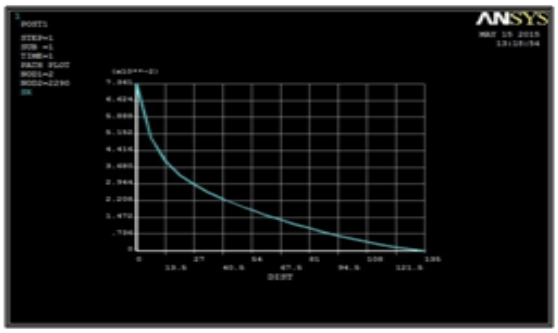

Figure 3: Variation of radial stress for uniform disk

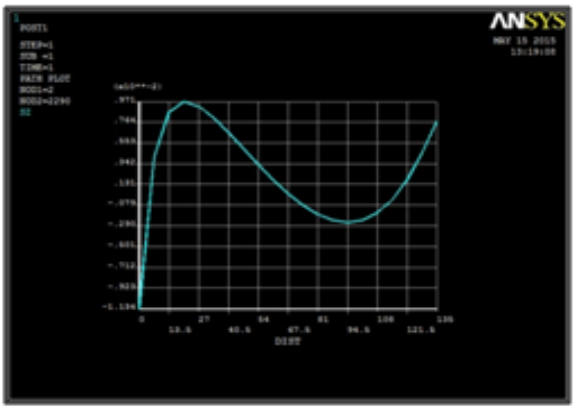

Figure 4: Variation of circumferential stress for uniform disk

2. Linearly varying disk

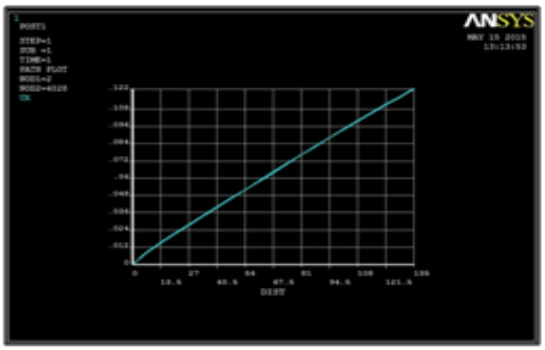

Figure 5: Variation of radial displacement for linearly varying disk

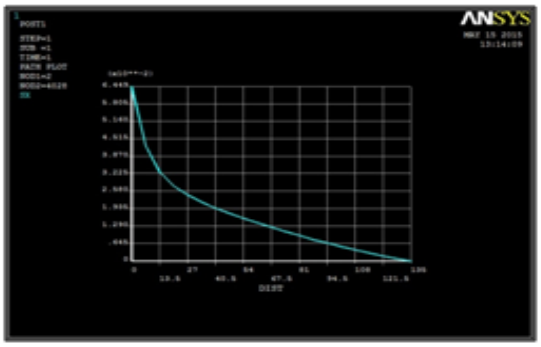

Figure 6: Variation of radial stress for linearly varying disk

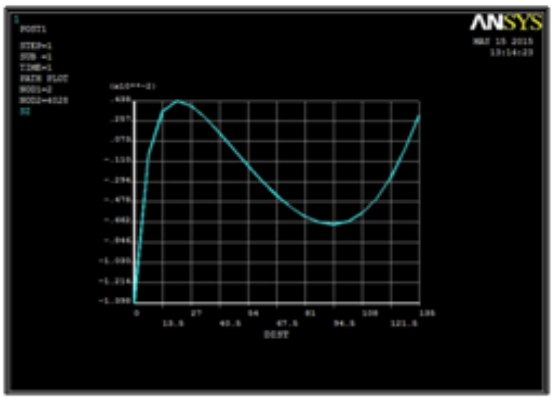

Figure 7: Variation of circumferential stress for linearly varying disk

ISSN (ONLINE): 2250-0758, ISSN (PRINT): 2394-6962

3. Convex disk

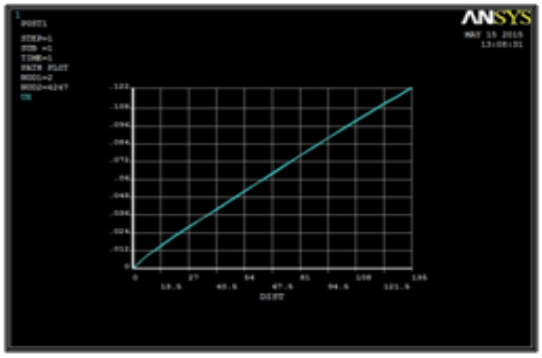

Figure 8: Variation of radial displacement for convex disk

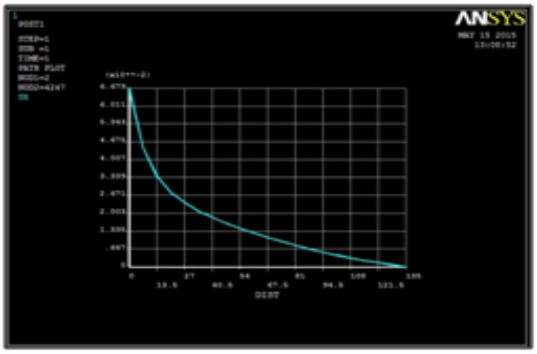

Figure 9: Variation of radial stress for convex disk

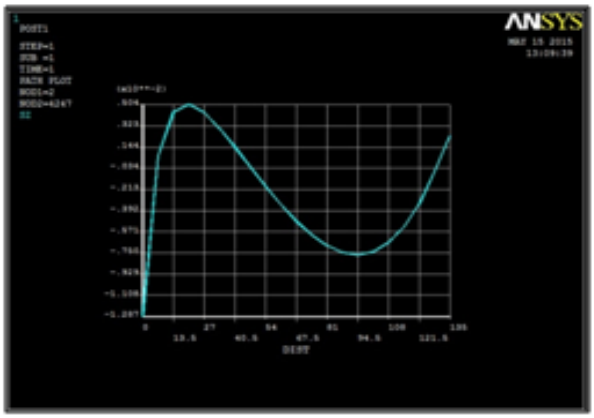

Figure 10: Variation of circumferential stress for convex disk

4. Concave disk

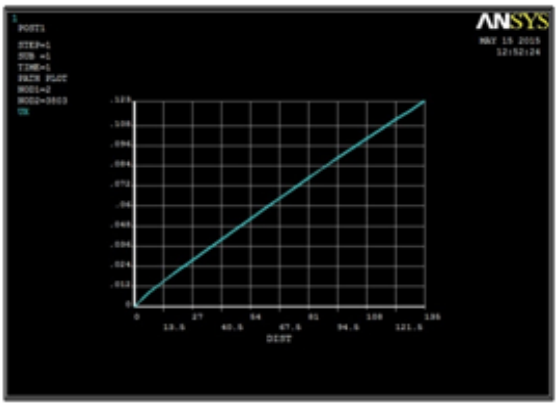

Figure 11: Variation of radial displacement for concave disk

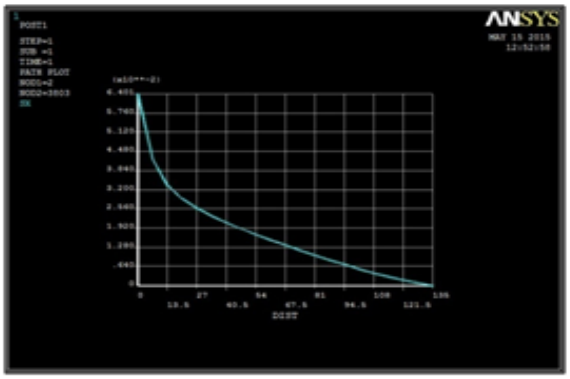

Figure 12: Variation of radial stress for concave disk

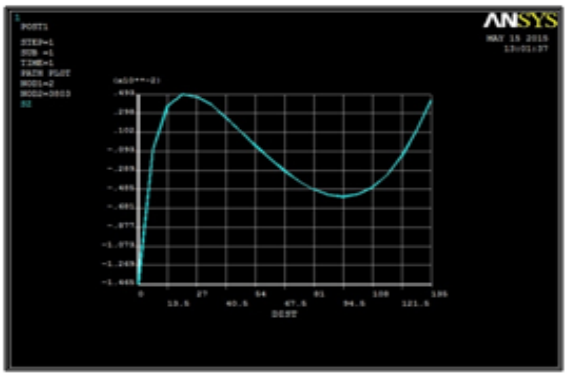

Figure 13: Variation of circumferential stress for concave disk

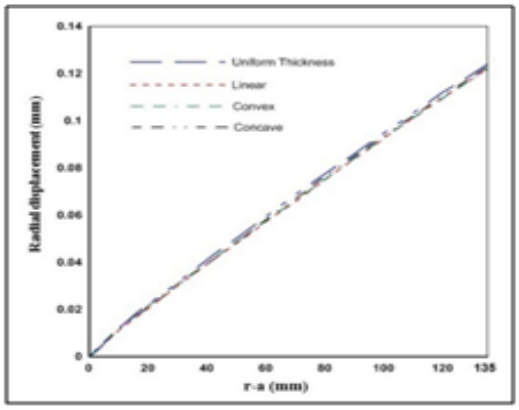

Figure 14: Comparison of radial displacement

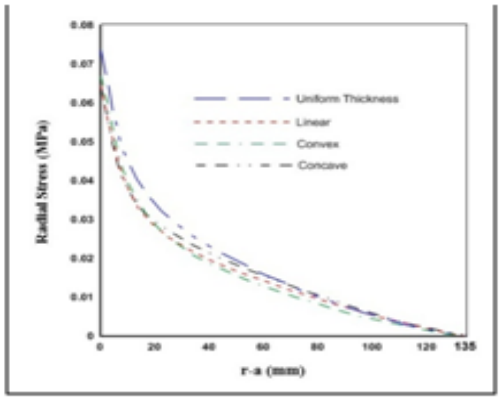

Figure 15: Comparison of radial stress

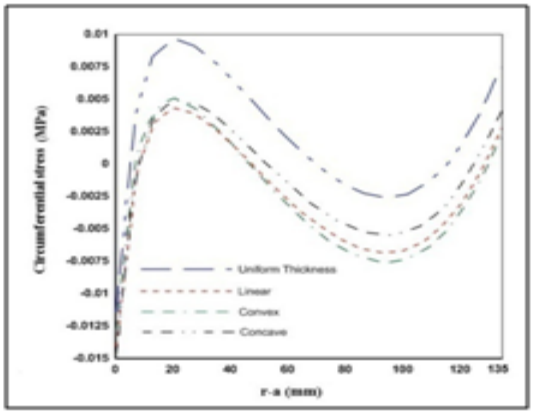

Figure 16: Comparison of circumferential stress

From Fig. 14 it is found that Uniform thickness disk has a little high radial displacement as compared to variable thickness. Thickness of the disk has a very little effect on the radial displacement. Radial displacement varies approximately linear from inner radius to outer radius. At inner radius it is minimum that is 0 and maximum at outer radius for all thickness profile. This is due to fix boundary condition at inner radius and free boundary condition at outer radius. Maximum value of the radial displacement for uniform thickness disk is 0.123 mm while for variable thickness disk (convex, concave and linear profile) its maximum value is 0.119 mm.

Radial stress is maximum at inner radius while minimum at outer radius, which confirms the constrained boundary conditions, applied. For linear temperature field Maximum radial stress in uniform thickness disk is 0.074 MPa, then convex disk has second highest value which is 0.067 MPa, then linear disk has 0.065 MPa and concave disk has 0.064 MPa maximum radial stresses.

Circumferential stress induced in the disks are tensile and compressive both in nature. Magnitude of the compressive stress is higher than the tensile stress. For linear temperature field maximum compressive stress is at inner radius and maximum tensile stress is at 50 mm radius. The value of maximum compressive stress is 0.015 MPa for all thickness profile. The value of maximum tensile stress is 0.009 MPa for uniform thickness disk, 0.005 for convex as well as concave disk and 0.004 for linear profile disk.

VI. CONCLUSION

In this work rotating disks of various thickness profiles made up of functionally graded material is analyzed. The disks have exponentially varying material properties and subjected to mechanical as well as thermal body forces. Problem was analyzed by finite element method in ANSYS Mechanical APDL. From the comparison of FGM disk and homogeneous disk (Fig. 1.) it can be observed that the maximum radial stress for a homogeneous disk is 10 MPa approximate while for FGM disk it is 7 MPa. Therefore FGM disk have advantage of reduction in maximum radial stress over the homogeneous material disk while by comparing uniform thickness disk and variable thickness disk (Fig. 14, Fig. 15 and Fig. 16) it can be concluded that there is great advantage of reduction in maximum values of displacement and stresses in variable thickness disks over uniform thickness disk.

REFERENCES

[1] J.N. Sharma, Dinkar Sharma, Sheo Kumar: Stress and strain analysis of rotating FGM thermoelastic circular disk by using FEM. International Journal of Pure and Applied Mathematics, Vol. 74 No. 3, 2012, 339-352.
[2] Hasan Callioglu, Metin Sayer, Ersin Demir: Stress analysis of functionally graded discs under mechanical and thermal loads. IJEMS, Vol. 18, april 2011, 111-118.
[3] Hasan Callioglu: Stress analysis in a functionally graded disc under mechanical loads and a steady state temperature distribution. Indian Academy of Sciences. Vol. 36, Part 1, February 2011, 53–64.
[4] Ashraf M. Zenkour, Daoud S. Mashat: Stress function of a rotating variable-thickness annular disk using exact and numerical methods. Scientific research publication, Engineering, Vol. 3, 2011, 422-430
[5] Hassan Zafarmand, Mehran Kadkhodayan: Nonlinear analysis of functionally graded nanocomposite rotating

thick disks with variable thickness reinforced with carbon nanotubes. Aerospace Science and Technology, Vol. 41, 2015, 47–54.
[6] Mohammad Zamani Nejad, Parisa Fatehi: Exact elastoplastic analysis of rotating thick-walled cylindrical pressure vessels made of functionally graded materials. International Journal of Engineering Science Vol. 86, 2015, 26–43.
[7] Hassan Zafarmand, Behrooz Hassani: Analysis of two-dimensional functionally graded rotating thick disks with variable thickness. Acta Mech 225, 2014, 453–464.
[8] M. Shariyat and R.Mohammadjani: Three-dimensional compatible finite element stress analysis of spinning two-directional FGM annular plates and disks with load and elastic foundation nonuniformities. LAJSS, Vol. 10, 2013, 859 – 890.
[9] J.N. Sharma, Dinkar Sharma, Sheo Kumar: Analysis of Stresses and Strains in a Rotating Homogeneous Thermoelastic Circular Disk by using Finite Element Method. International Journal of Computer Applications. Vol. 35, No.13, December 2011, 0975 – 8887.
[10] J.S. Faragher and R.A. Antoniou: Preliminary Finite Element Analysis of a Compressor Disk in the TF30 Engine. DSTO Aeronautical and Maritime Research Laboratory, Melbourne Victoria 3001 Australia (2000).
[11] P. Seshu: a text book of finite element analysis. PHI Learning Pvt. Ltd. 01-Jan-2003.
[12] Ashraf M. Zenkour, Daoud S. Mashat: Analytical and Numerical Solutions for a Rotating Annular Disk of Variable Thickness. Scientific research publication, Applied Mathematics, 1, 2010, 431-438.
[13] Abdur Rosyid, Mahir Es-Saheb and Faycal Ben Yahia: Stress Analysis of Nonhomogeneous Rotating Disc with Arbitrarily Variable Thickness Using Finite Element Method. Research Journal of Applied Sciences, Engineering and Technology 7(15): 3114-3125, 2014.